Optimized Acquisition Time and Image Sampling for Dynamic SPECT of Tl-201

Chi-Hoi Lau, Stefan Eberl, *Member, IEEE*, Dagan Feng,* *Senior Member, IEEE*, Hidehiro Iida, Pak-Kong Lun, Wan-Chi Siu, *Senior Member, IEEE*, Yoshikazu Tamura, George J. Bautovich, and Yukihiko Ono

***Abstract*— With the recent development in scatter and attenuation correction algorithms, dynamic single photon emission computerized tomography (SPECT) can potentially yield physiological parameters, with tracers exhibiting suitable kinetics such as thallium-201 (Tl-201). A systematic way is proposed to investigate the minimum data acquisition times and sampling requirements for estimating physiological parameters with quantitative dynamic SPECT.**

Two different sampling schemes were investigated with Monte Carlo simulations: 1) Continuous data collection for total study duration ranging from 30–240 min. 2) Continuous data collection for first 10–45 min followed by a delayed study at approximately 3 h. Tissue time activity curves with realistic noise were generated from a mean plasma time activity curve and rate constants $(K_1 - k_4)$ derived from Tl-201 kinetic studies in 16 dogs. Full dynamic sampling schedules (DynSS) were compared to optimum sampling schedules (OSS).

We found that OSS can reliably estimate the blood flow related K_1 and V_d comparable to DynSS. A 30-min continuous collection was sufficient if only K_1 was of interest. A split session schedule of a 30-min dynamic followed by a static study at 3 h allowed reliable estimation of both K_1 and V_d avoiding the need for a prolonged (>60-min) continuous dynamic acquisition. The methodology developed should also be applicable to optimizing sampling schedules for other SPECT tracers.

***Index Terms*—Compartmental modeling, optimum image sampling schedule, SPECT, Tl-201 tracer kinetics.**

Manuscript received February 6, 1997; revised April 27, 1998. This research was supported in part by grants from the Australian Research Council (ARC) and UGC, and by the Ministry of Health and Welfare, Japan, under a research grant for cardiovascular diseases (8C-5). The Associate Editor responsible for coordinating the review of this paper and recommending its publication was R. Leahy. *Asterisk indicates corresponding author.*

C.-H. Lau is with the Biomedical and Multimedia Information Technology Group, Department of Computer Science, University of Sydney, Sydney, NSW, 2006, Australia. He is also with the Department of Electronic Engineering, Hong Kong Polytechnic University, Hong Kong.

S. Eberl is with Department of PET and Nuclear Medicine, Royal Prince Alfred Hospital, Sydney, NSW, 2050, Australia. He is also with the Biomedical and Multimedia Information Technology Group, Department of Computer Science, University of Sydney, Sydney, NSW, 2006, Australia.

*D. Feng is with the Biomedical and Multimedia Information Technology Group, Department of Computer Science, University of Sydney, Sydney, NSW, 2006, Australia. (e-mail: feng@staff.cs.usyd.edu.au). He is also with the Department of Electronic Engineering, Hong Kong Polytechnic University, Hong Kong.

H. Iida, Y. Tamura, and Y. Ono are with the Department of Radiology and Nuclear Medicine, Research Institute for Brain and Blood Vessels, Akita 010 Japan.

P.-K. Lun and W.-C. Siu are with the Department of Electronic Engineering, Hong Kong Polytechnic University, Hong Kong.

G. J. Bautovich is with the Department of PET and Nuclear Medicine, Royal Prince Alfred Hospital, Sydney, NSW 2050, Australia.

Publisher Item Identifier S 0278-0062(98)06455-6.

I. Introduction

DYNAMIC single photon emission computed tomography (SPECT) and recent advances in attenuation and scatter correction have opened the possibility of quantifying physiological parameters with SPECT and tracers with suitable kinetics. Recently, Iida *et al* have shown that absolute regional cerebral blood flow and volume of distribution can be calculated using dynamic Iodine-123 (I-123) SPECT and compartmental modeling [1], [2]. Similarly, Onishi *et al* have applied dynamic SPECT to estimate receptor binding [3]. Technetium-99m (Tc-99m) teboroxime has been suggested for measuring myocardial blood flow. Teboroxime exhibits fast kinetics, which makes it unsuitable for traditional static SPECT imaging, but is well suited to estimating physiological parameters with short, fast dynamic acquisitions [4], [5]. Iida *et al.* have demonstrated the feasibility of estimating myocardial blood flow with thallium-201 (Tl-201) dynamic SPECT, which exhibits much slower kinetics, more in line with typical SPECT tracers [6].

While dynamic SPECT studies have only recently gained increased attention, dynamic positron emission tomography (PET) studies and compartmental modeling are well established. Great attention has been paid to the design of PET image frame sampling schedules to increase the quantitative accuracy. Hawkins *et al.* [7] studied the effects of temporal sampling on the glucose model using 18-fluoro-deoxy-D-glucose (FDG) and Mazoyer *et al.* [8] proposed a general method for estimating the precision of parameters resulting from the use of various experimental designs, including the rate of tomographic data collection. Delforge *et al.* [9] applied an experimental design optimization framework and various criteria to the estimation of receptor-ligand reaction model parameters with dynamic PET data. Jovkar *et al.* [10] addressed the general problem of finding an optimized scan schedule in PET dynamic studies which minimizes the parameter estimation errors. They found that there is a monotonic improvement in the index of parameter accuracy with increasing sampling frequency and concluded that a higher sampling frequency (more image samples), particularly in the early stage, should be used. We have recently demonstrated that the above conclusion was mainly due to using a cost function based on assuming that sample points represent instantaneous activity concentration at the sample time, while in fact each sample point represents the integral of the changing activity concentration over the duration of the collection frame. The assumption of instantaneous sample points introduces increasing errors with increasing

frames times, which prevents the reduction of the image frame numbers without adversely affecting accuracy. We therefore used a modified cost function based on integrated activity concentration for PET modeling [11], and have shown that by combining several adjacent image frames, the resultant smaller number of image frames can produce a comparable parameter estimation accuracy. The optimum sampling schedule (OSS) technique provides a formalized methodology for determining the acquisition times of the minimum number of frames required to describe the selected kinetic model [12]–[15]. Based on this approach, we have recently investigated OSS for PET input function [16], PET output function [14], and whole-body PET image acquisition [17].

With the exception of Chatziioannou *et al.* [18], who performed some systematic analysis of total scan time as part of their data processing schemes to reduce noise, little attention has been paid to systematically investigate the total scan duration. Instead total scan duration is usually decided empirically based on the following factors:

1) physical and physiological half life of the radiotracer;
2) existence of blood metabolites;
3) model consideration, (For example the C-11 acetate model is only validated for the initial 15–20 min);
4) clinical consideration to keep the scan as short as possible for the convenience of patients.

Clinical practicality is a particularly important consideration for dynamic SPECT sampling schedules. The slow kinetics of typical SPECT tracers may require unrealistically long total acquisition times to obtain reliable estimation of the slower rate constants. As shown by Iida *et al*, the number of frames and total time patient is in the scanner can be reduced by separating the study into two scanning sessions and assuming a single tissue compartment model [1], [2]. Alternatively, some of the rate constants or their ratios can be set to fixed values to simplify the model and provide more reliable parameter estimation with limited data [19]. However, these assumptions may not be generally applicable to all SPECT tracers and a generally applicable methodology for optimizing sampling within the constraints imposed by dynamic SPECT would be of benefit.

The aims of this study were as follows:

1) systematically investigate the reliability of parameter estimation as a function of total acquisition time;
2) determine the minimum required continuous dynamic SPECT acquisition time for the relatively slow kinetics of Tl-201;
3) determine if there was a critical acquisition time length, beyond which little improvement in reliability is achieved;
4) investigate a clinically practical alternative to prolonged continuous dynamic acquisitions;
5) determine if the reduced frames of OSS can provide similar accuracy as full dynamic acquisition for dynamic SPECT studies.

While this study concentrated on applying the methodology to Tl-201 kinetics, the methodology developed here should also be applicable to other dynamic SPECT studies.

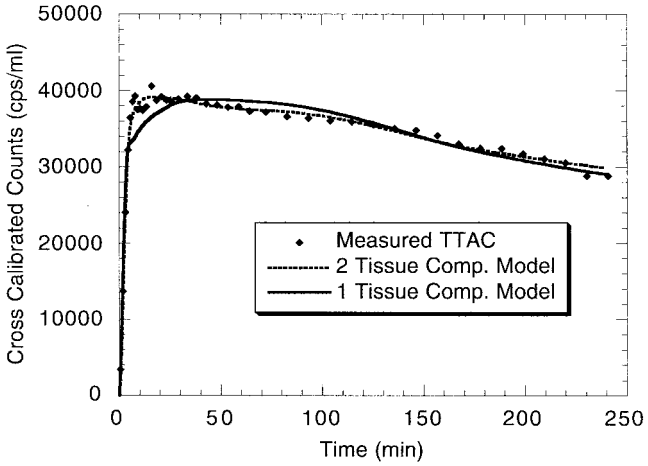

Fig. 1. Measured TTAC from one of the dynamic SPECT dog studies fitted with one- and two-tissue compartment models. The two-tissue compartment model provides a visually better fit to the measured TTAC than the one-tissue compartment model. TTAC's have been cross calibrated to the well counter used to count plasma samples and, thus, have units of cps/ml.

II. Materials and Method

A. Simulations of Tissue Time Activity Curves (TTAC's)

Simulated TTAC's were derived from rate constants estimated from dynamic Tl-201 SPECT studies in 16 dogs. The dog studies were carried out as follows: The dogs were anaesthetized and positioned on a dual head gamma camera (Toshiba GCA7200). A transmission study was carried out using a line source at the focus of a fan beam collimator. The dynamic SPECT study was initiated at the start of a 3-min infusion of 110 MBq of Tl-201. Frequent arterial blood samples were drawn throughout the dynamic study. The detectors rotated continuously completing a 360° acquisition every 15 s. The 15-s frames were added on-line to provide the following 42-frame dynamic sequence for resting studies: 10×1 min, 6×2 min, 3×4 min, 5×5 min, and 18×10 min for a total acquisition time of 4 h. Studies were also carried out in dogs with increased blood flow achieved by constant infusion of adenosine and reduced blood flow produced by beta-blockers. The total study duration for the adenosine and beta-blocker studies was limited to 1 h.

Tl-201 data were corrected for scatter using transmission dependent scatter correction [20]–[22] and reconstructed with the ordered-subset expectation-maximization algorithm (OSEM) [23] using transmission-data-based measured attenuation correction. The reconstructed SPECT pixel values were cross calibrated with a separate uniform phantom study to the well counter used to count the plasma samples for deriving the input function. Thus the SPECT voxel values were in the same units as the plasma samples (cps/ml), which is a basic requirement for compartmental modeling. Regions of interest (ROI's) were drawn on a central slice through the myocardium for anterior, lateral, apical, septal and inferior myocardial areas and TTAC's were generated and again expressed in the cross calibrated well counter units of cps/ml. Each of the TTAC's were individually fitted with one- and two-tissue compartment models using nonlinear least-square fitting (Fig. 1).

TABLE I
THE FOUR RATE CONSTANTS $(K_1 - k_4)$ AND THE VOLUME OF DISTRIBUTION (V_d) FOR THE FIVE SELECTED PARAMETER SETS. UNITS FOR THE RATE CONSTANTS ARE min-1

	K_1	k_2	k_3	k_4	V_d
Set 1	0.68080	0.90024	0.14529	0.04136	34.1264
Set 2	0.72961	0.03595	0.04151	0.01554	74.5205
Set 3	0.18749	0.02068	0.06021	0.02004	36.3078
Set 4	0.25643	0.08405	0.25912	0.00926	88.3939
Set 5	1.51312	0.19493	0.28104	0.06796	39.8610

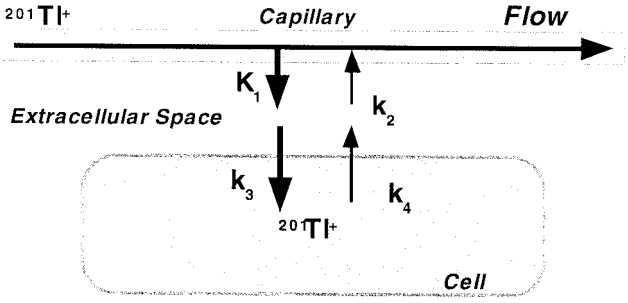

Fig. 2. Assumed compartmental model for Tl-201 with two tissue compartments: extracellular and intracellular compartment.

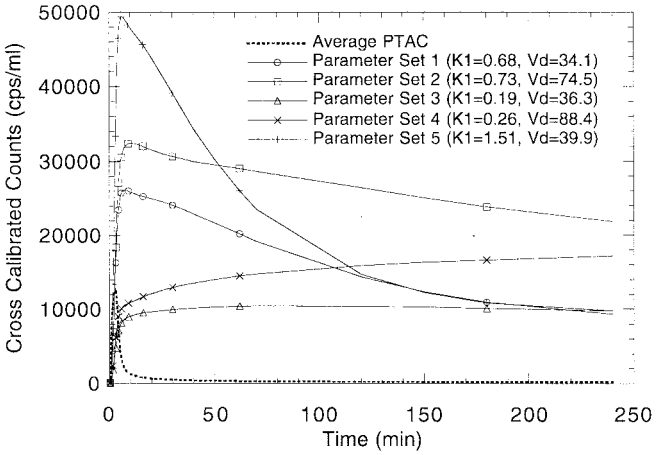

Fig. 3. The average PTAC and the five noise-free TTAC's for the five selected parameter sets. TTAC's are assumed to be cross calibrated to plasma curve and, thus, have the same units as plasma curve (cps/ml).

From the results of the compartmental fitting, the two-tissue compartment [extracellular and intracellular Tl-201 compartments (Fig. 2)] model was assumed for the simulations. This model is also in line with recent literature reports [24]. K_1 is the influx constant and is proportional to blood flow for a flow limited tracer like Tl-201. Other rate constants are as shown in Fig. 2. TTAC's were generated for the five selected sets of rate constants $(K_1 - k_4)$ given in Table I. Rate constant sets were selected to cover a range of flow conditions. Set 1 represents mean rate constants from all 16 dogs, set 2 is from a dog with resting flow, sets 3 and 4 from dogs with reduced flow induced by constant beta-blocker infusion and flow for set 5 was increased by constant adenosine infusion over the study duration.

The derived volume of distribution macro parameter (V_d) given by

$$\text{Volume of Distribution} = \frac{K_1 * (k_3 + k_4)}{k_2 * k_4} \tag{1}$$

is also shown in Table I. Of particular interest were the influx rate constant K_1, which is related to blood flow $(K_1 = \text{flow} * \text{extraction fraction})$ and V_d, which is related to the cells' ability to concentrate Tl-201, an important indicator for viability. For each set of rate constants, time activity curves were generated by convolving the compartmental model function with the plasma time activity curve (PTAC) derived from the average of the 16 dogs (Fig. 3).

While projection data can be expected to follow Poisson noise (before scatter correction), this is unlikely to be the case for reconstructed data. However, variance can still be expected to change for different collection times and activities. To investigate noise variance for our quantitative reconstruction method (OSEM with attenuation and scatter correction), a uniform phantom was collected dynamically and processed identically to the dog data. This indicated that the variance increased approximately proportional to the frame time (i.e., increase of frame time by factor of four increased variance by approximately a factor of four) and conversely, variance increased proportional to the activity in the phantom. Thus, we estimate noise variance for a particular TTAC point using the following expression:

$$\text{Noise Variance} = C * y(t_k)/\Delta t(t_k) \tag{2}$$

where C is a constant to give a specified noise level. Five different noise levels were investigated with $C = 2$, 10, 23, 41, and 65. $y(t_k)$ is the average TTAC curve value measured at the kth time interval at mid scan time t_k and $\Delta t(t_k)$ is the length of the kth time interval. A simulated TTAC with $C = 65$ is shown in Fig. 4 together with the corresponding measured TTAC curve from the dog ROI analysis. The estimated noise coefficient of variation (CV) near the peak counts, and for 1-min samples ranged from 1.8%–9.2% for the simulations with $C = 2$–65, respectively. Estimated noise CV for the measured TTAC was approximately 3%–5%, corresponding approximately to a noise constant between $C = 10$ and $C = 23$. The noise was assumed to have a Gaussian distribution, in line with experience with PET TTAC's [25], and a variance given by (2). The Gaussian noise was generated and added to the TTAC points using the algorithm described in [26, ch. 7]. The same noise model was used to estimate parameter estimation reliability when fitting that compartmental model to the measured dog data and was found to be in good agreement with reliability estimates which do not require a noise model to be specified, providing further indirect support for our chosen noise model.

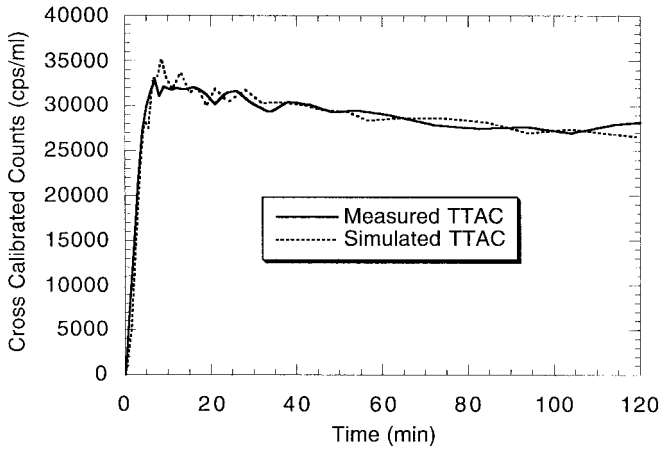

Fig. 4. A measured TTAC (solid line) and corresponding simulated TTAC (dashed line) with noise constant $C = 65$. TTAC's have been cross calibrated to the well counter used to count plasma samples and, thus, have units of cps/ml.

B. Optimum Sampling Schedule

The OSS technique provides a mechanism to maximize the information matrix M and, conversely, to minimize the covariance matrix (COVAR) of the estimated parameters by rearranging the sample intervals, based on the minimum number of required samples, and a given total study duration and model [12]–[15]. According to the Cramer–Rao theorem, the covariance matrix of an unbiased estimate $\hat{p}$ of the parameter vector p is lower bounded by the inverse of M, i.e.,

$$\text{COVAR}(\hat{p}) \geq M^{-1}.$$

Since the determinant of COVAR($\hat{p}$) is proportional to the volume of the parameter confidence region [27], it provides a criterion for discriminating between various experimental protocols. The sampling schedule is adjusted iteratively to maximize the determinant of M (det(M)) as follows: Starting with the full dynamic sampling schedule, at each iteration, each interval is adjusted in turn in the direction which increases the det(M) of the parameter estimates for the TTAC resampled with the adjusted interval. Adjusting interval k will also adjust interval $k+1$ by the same amount, but in the opposite direction to maintain the same total collection time and avoid overlap. When the length of an interval falls below a set value (10 s in this study), it is merged with the next interval. The iterations are repeated until det(M) converges to a specified tolerance. The OSS will depend on the exact shape of the TTAC. As this is unknown prior to the measurement, OSS derived for TTAC simulated from parameter set 1 (Table I) was used for all other parameter sets to investigate the applicability of a single OSS scheme to a range of Tl-201 kinetics.

The OSS methodology was also employed to find optimum sampling based on two sessions of scanning: A short (10–45 min) multiframe acquisition immediately post tracer injection and a delayed single frame acquisition. The timing for the delayed frame was determined by adjusting the mid-scan time of the minimum number of required frames with fixed duration of 10 min within an overall time period of 240 min until again det(M) was maximized. This resulted in a mid scan time of 173 min for the last time point. A single 10-min frame was then fixed at 173 min and OSS technique was then applied to determine the sampling requirements for the first session. Sampling schedules were derived for total first-session acquisition times ranging from 10 to 45 min. This scheme is similar to current clinical studies, where an acquisition is performed soon after Tl-201 injection, followed by a redistribution study at around 3–4 h. Thus, the following OSS's were investigated.

1) Continuous data collection over the whole study duration (i.e., single session of scanning) ranging from 30 to 240 min, which is the conventional OSS approach.
2) Initial data collection for a shorter period (10–45 min) accompanied by a delayed study at 173 min (i.e., two sessions of scanning).

C. Evaluation of OSS

The CV and error in estimating the parameters were evaluated for both the continuous one-session and two-session optimum sampling schemes (OSS-1) and (OSS-2), respectively, and compared to conventional full dynamic sampling (as used in the original dog studies) for both the continuous (DynSS-1) and the two-session sampling schemes (DynSS-2) using Monte Carlo simulation technique as follows.

1) For each selected parameter set, noiseless TTAC's were generated by convolving the compartmental model function with the PTAC, according to the different sampling schedules.
2) Noise was then added to the noiseless TTAC's at the five noise levels according to (2). For each noise level, 100 curves were generated using different noise seeds.
3) Rate constants were estimated with nonlinear least square curve fitting from the simulated data. The modified cost function [14], based on integrating the instantaneous count rates over the frame duration, was used for the fitting. The fitted rate constants were constrained to be positive.
4) CV's were determined for each parameter from the 100 curve fits. Error was calculated by comparing the mean fitted parameters to the known parameter values used for generating the TTAC's.

III. Results

A. Optimum Sampling Schedule

Table II shows the OSS-1 as well as the DynSS-1. It should be noted that for different study durations, the number of samples for DynSS-1 ranged from 18 samples for 30 min to 42 samples for 4 h. For OSS-1, there were only four samples, which is the minimum number of samples required for the four parameters $(K_1 - k_4)$ used in the model [15]. Table III shows the sampling schedule for OSS-2 and DynSS-2, using the same notation as Table II. The schedules taken in different sessions are separated by square brackets. The results of the optimized intervals are shown in the right column of the table and the optimized mid-scan time for the second session was 173 min post-injection.

TABLE II
SAMPLING SCHEDULES FOR SINGLE SESSION OF SCANNING. THE LEFT, MIDDLE, and RIGHT COLUMNS SHOW THE TOTAL STUDY DURATION, THE SAMPLING SCHEDULES OF THE DynSS-1, AND OSS-1, RESPECTIVELY. THE FIRST ENTRY "10 × 1 MIN" IN THE MIDDLE COLUMN MEANS THAT 10 SAMPLES, EACH 1-MIN LONG, WERE TAKEN

Total Length	DynSS-1	OSS-1
30 min	10x1 min, 6x2 min, 2x4 min	1x5 min, 1x7 min, 1x11 min,1x6 min
45 min	10x1 min, 6x2 min, 3x4 min, 2x5 min	1x5 min, 1x5 min, 1x18 min, 1x11 min
60 min	10x1 min, 6x2 min, 3x4 min, 5x5 min	1x5 min, 1x10 min, 1x25 min, 1x19 min
90 min	10x1 min, 6x2 min, 3x4 min, 5x5 min, 3x10 min	1x5 min, 1x10 min, 1x38 min, 1x36 min
120 min	10x1 min, 6x2 min, 3x4 min, 5x5 min, 6x10 min	1x6 min, 1x11 min, 1x48 min, 1x54 min
150 min	10x1 min, 6x2 min, 3x4 min, 5x5 min, 9x10 min	1x6 min, 1x11 min, 1x57 min, 1x75 min
180 min	10x1 min, 6x2 min, 3x4 min, 5x5 min, 12x10 min	1x6 min, 1x11 min, 1x63 min, 1x99 min
210 min	10x1 min, 6x2 min, 3x4 min, 5x5 min, 15x10 min	1x6 min, 1x12 min, 1x68 min, 1x124 min
240 min	10x1 min, 6x2 min, 3x4 min, 5x5 min, 18x10 min	1x6 min, 1x12 min, 1x71 min, 1x151 min

TABLE III
SAMPLING SCHEDULES FOR TWO SESSIONS OF SCANNING USING THE SAME NOTATION AS IN TABLE II. THE SAMPLES TAKEN AT DIFFERENT SESSIONS ARE SEPARATED BY SQUARE BRACKETS. THE FIRST SESSION IS TAKEN IMMEDIATELY AFTER TRACER INJECTION AND THE SECOND SESSION IS TAKEN AT 173 MIN POST INJECTION

Protocol	DynSS-2	OSS-2
(A)10 min+10 min	[10x1 min],[1x10 min]	[1x4 min, 1x4 min, 1x2 min],[1x10 min]
(B)20 min+10 min	[10x1 min, 5x2 min],[1x10 min]	[1x5.5 min, 1x7.5 min,1x7 min],[1x1 0min]
(C)30 min+10 min	[10x1 min,6x2 min,2x4 min],[1x10 min]	[1x5 min,1x 8 min, 1x17 min],[1x10 min]
(D)45 min+10 min	[10x1 min,6x2 min,3x4 min,2x5 min],[1x10 min]	[1x5 min, 1x10 min, 1x30 min],[1x10 min]

B. Percentage Errors and CV—Single-Session Scanning

The percentage error for the fitted parameters was calculated by comparing them to the known parameter values used for the simulation. CV was estimated from the variation of parameters over the 100 Monte Carlo simulation runs. The percentage error and CV of estimated K_1, k_2, k_4, and V_d for set 1 at the five noise levels are plotted as a function of total study duration for DynSS-1 in Fig. 5 and for OSS-1 in Fig. 6. Curves for k_3 were very similar to those of k_2 and are, thus, not shown. Little systematic change in either percentage error or CV of K_1 is observed as the length of collection time increased from 30 min to 4 h. As the length of collection time increased, both percentage error and CV for k_2, k_3, k_4, and V_d tended to decrease to a plateau at 60–90 min for both DynSS-1 and OSS-1. Before the plateau, the percentage error increased with the noise level. Little effect of noise on percentage error was observed after the plateau. In contrast, CV was influenced by noise level for all study duration. CV for OSS-1 and DynSS-1 were very similar as were the percentage errors for parameters K_1, k_4, and V_d. However, percentage errors for k_2 and k_3 were more than twice as large for OSS-1 than for DynSS-1.

Fig. 7 is a comparison of the percentage error and CV of the estimated K_1 at different total study duration, for different parameter sets using DynSS-1 or OSS-1. These curves are the average of the results obtained at the different noise levels. The figures show that the percentage error and CV are all below 4% and 11%, respectively. Both percentage error and CV do not decrease as the total time length is increased, i.e., K_1 estimation is not improved by extending the scanning time. Therefore, a 30-min scanning session is sufficient if only the blood-flow indicator K_1 is of interest.

Fig. 8 shows the percentage error and CV of the estimated V_d at different total time lengths of scanning, for different parameter sets and for both DynSS-1 and OSS-1. There is a marked improvement in both percentage error and CV as the scanning time is increased from 30 to 120 min. Thereafter, both percentage error and CV plateau. To obtain a less than 20% error and CV for V_d, a minimum scanning time length of 120 min is required, which may be reduced to 90 min, if somewhat higher CV of $<$30% is tolerated in low flow regions.

C. Percentage Errors and CV—Separate Scanning Sessions

An overall summary of K_1 and V_d estimation as a function of sampling schedule is shown in Figs. 9 and 10. For K_1 estimation, an initial 10–20-min dynamic in combination with a delayed sample or a single 30-min dynamic are sufficient. With addition of the delayed scan at approximately 3 h, the initial dynamic can be reduced to 30 min and still achieve similar accuracy and CV for V_d as a full 120-min scan. However, the 30-min dynamic plus 10-min delayed sample is considerably more practical in a routine clinical setting, being similar in acquisition times to current rest-redistribution protocols.

IV. DISCUSSION

In this study, we systematically investigated the reliability of parameter estimation as a function of acquisition time and applied the OSS technique to determine optimized, practical sampling schedules for dynamic Tl-201 SPECT. We found that: 1) OSS can provide reliable estimates of both K_1 and V_d, comparable to that of full dynamic sampling which often requires far more images. 2) K_1 can be estimated with a relatively short study duration of 30 min, while estimation of V_d requires at least 90–120 min to achieve acceptable precision, highlighting the need for careful selection of study duration to obtain reliable estimates of the parameters of interest. 3) Dividing the scanning into early and delayed sessions allowed accurate estimation of V_d, without requiring an unacceptably long collection time.

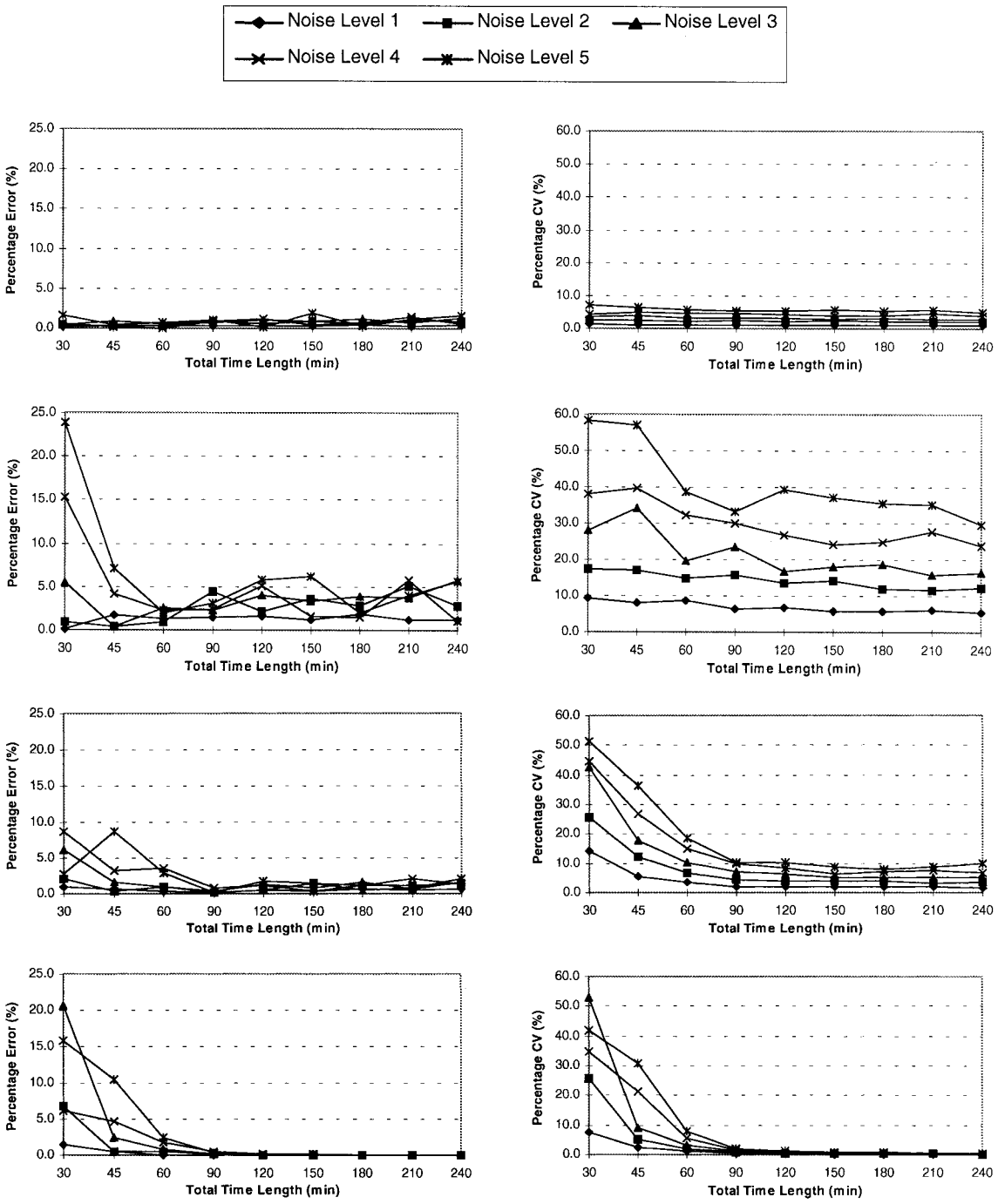

Fig. 5. (a) Percentage error and (b) CV of, from top to bottom, estimated K_1, k_2, k_4, and V_d as a function of total sampling time for DynSS-1. For each parameter, percentage error and CV are plotted at each of the five noise levels. Results are for parameter set 1. The same y-axis scale has been used for percentage error of all parameters and also for CV to facilitate comparison.

A. Comparison of DynSS and OSS

The OSS generally had a performance comparable to that of full dynamic sampling scheme for estimating K_1 and V_d. Only at very high K_1 (set 5) and low K_1 and high V_d (set 4) was there an appreciably increased CV of K_1 for OSS-1 compared with DynSS-1 (Fig. 7). However, the increase in CV was not excessive being in the order of 3%–4%. In contrast, OSS-1 could not successfully separate k_2 and k_3 rate constants. The percentage errors for these two rate constants using OSS-1 was more than double that of DynSS-1 (Figs. 5 and 6). Thus, if accurate estimates of k_2 and k_3 are required, DynSS-1 is the preferred sampling method.

The OSS substantially reduced the number of required SPECT acquisition frames to only four, irrespective of total acquisition time, compared with the 18–42 acquisition frames for the full dynamic study. As a result, it can significantly reduce the amount of dynamic image data (and, hence, the

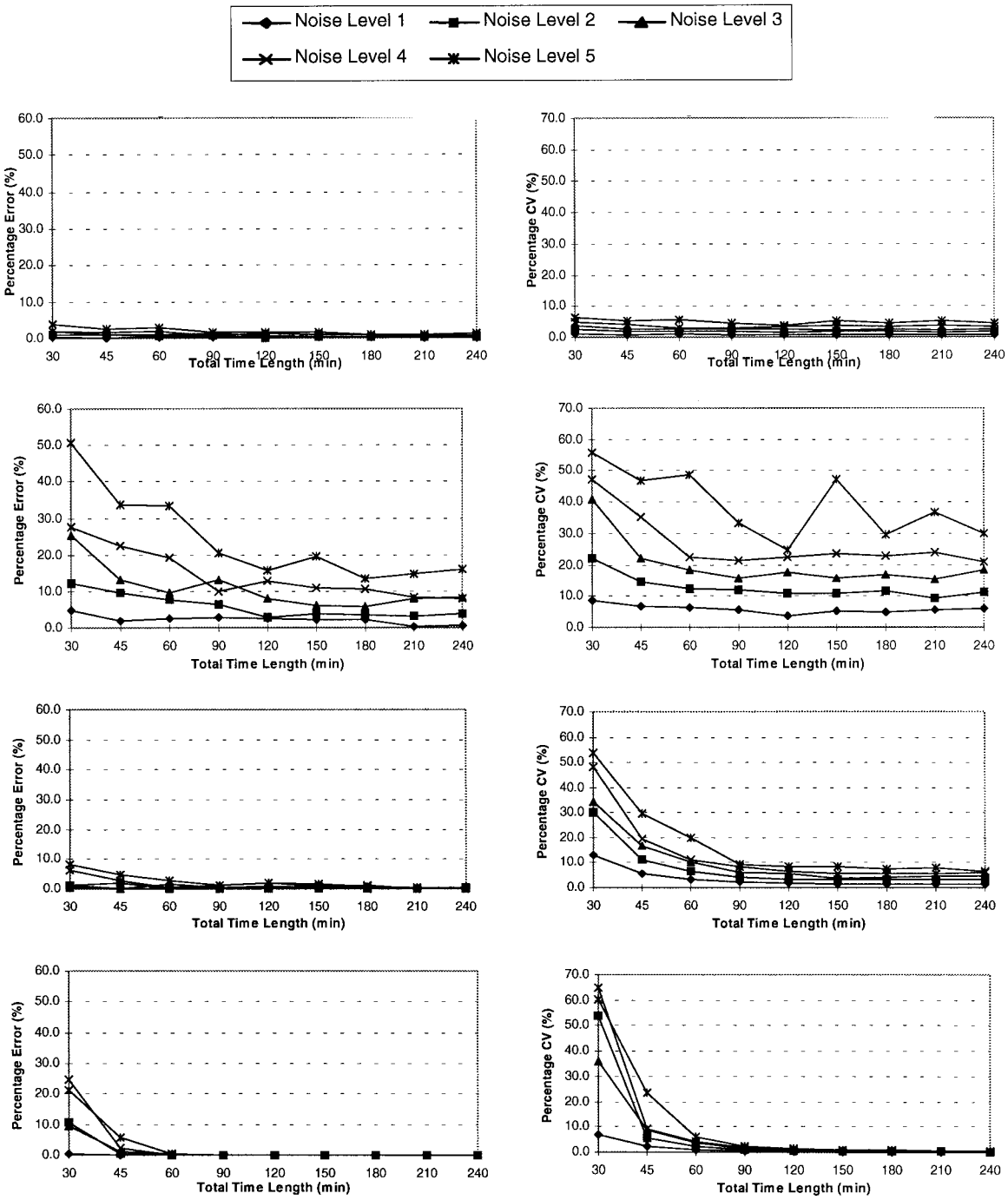

Fig. 6. (a) Percentage error and (b) CV of, from top to bottom, estimated K_1, k_2, k_4, and V_d as a function of total sampling time for OSS-1. For each parameter, percentage error and CV are plotted at each of the five noise levels. Results are for parameter set 1. The same y-axis scale has been used for percentage error of all parameters and also for CV to facilitate comparison.

storage space) and speed up the data analysis process in daily clinical applications. The shortest acquisition frame time for OSS was 5 min, compared to 1 min for the DynSS, which makes OSS dynamic SPECT readily implementable on existing SPECT systems.

B. Minimum Time for the Measurement of K_1 and V_d

For both OSS-1 and DynSS-1, we found that a 30-min scanning time length is sufficient for an accurate estimation of K_1 alone (Figs. 7 and 8). Prolonging the scanning time beyond 30 min produced no appreciable gain in accuracy or CV. For the 30-min study duration, percentage errors and CV for V_d were greater than 50% (Figs. 9 and 10). To obtain an accurate estimation for V_d, a 90–120-min study duration is necessary. This finding is not unexpected, as early uptake of Tl-201 is predominantly related to flow, thus the early dynamics are mostly determined by flow. However, the typically >30 ml/ml V_d of Tl-201, results in slow redistribution, particularly in low

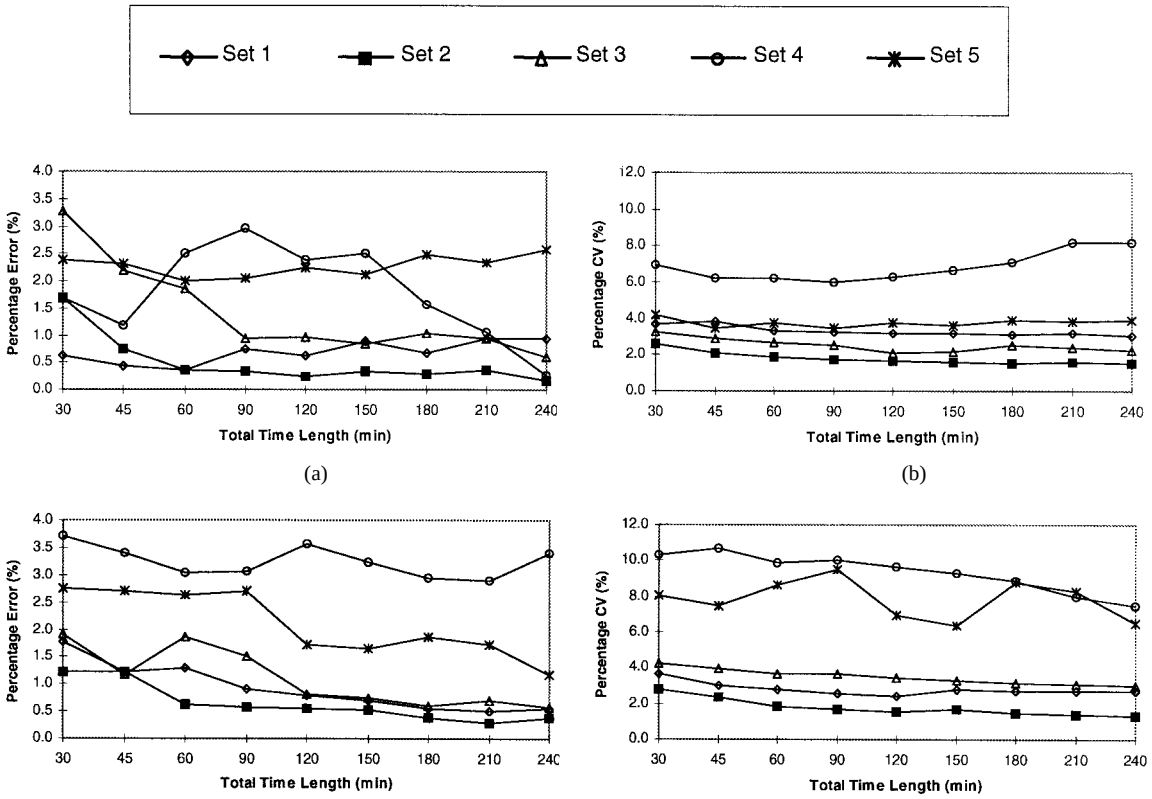

Fig. 7. Comparison of percentage error and CV for the estimated K_1 at different total time lengths for (a) and (b) full dynamic sampling schedule and (c) and (d) OSS. Set 1–Set 5 represent the five selected parameter sets.

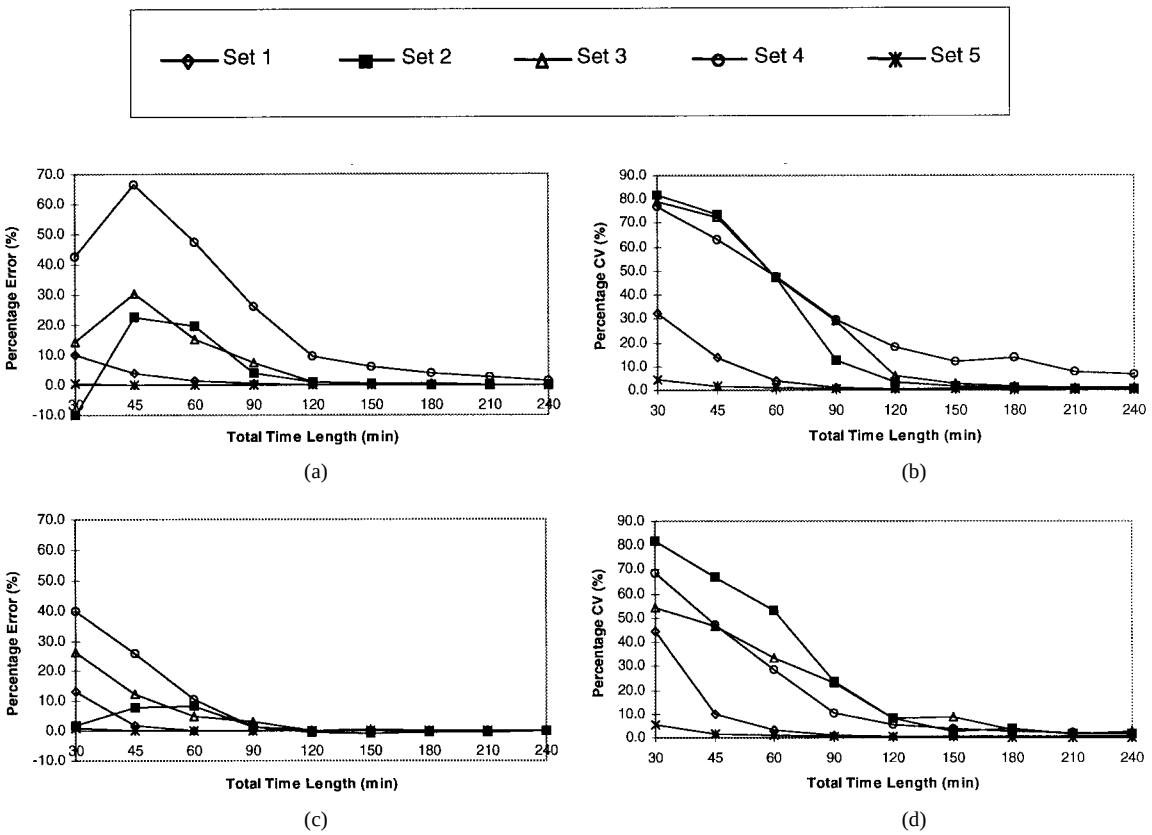

Fig. 8. Comparison of percentage error and CV of the estimated volume of distribution (V_d) at different total time lengths for (a) and (b) full dynamic sampling schedule and (c) and (d) OSS. Set 1–Set 5 represent the five selected parameter sets.

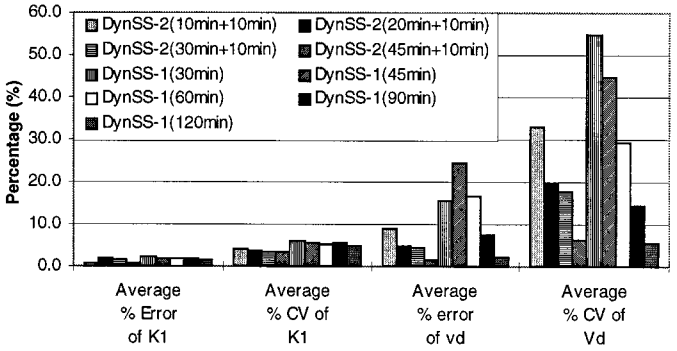

Fig. 9. Comparison of DynSS-2 and DynSS-1. The values inside the brackets are the length of the study duration. Average results of the five parameter sets are shown.

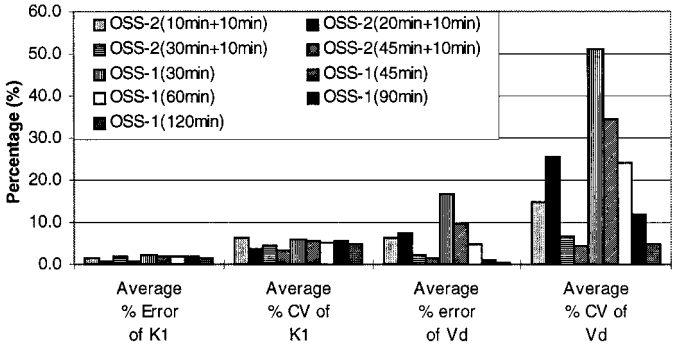

Fig. 10. Comparison of OSS-2 and OSS-1. The values inside the brackets are the length of the study duration. Average results of the five parameter sets are shown.

flow areas and, thus, a relatively long study duration is required to obtain reliable estimates of V_d.

For continuous data acquisition sampling schemes (OSS-1 and DynSS-1), patients would be required to remain in the camera for 90–120 min to obtain accurate estimates of V_d. This is clearly impractical for routine clinical studies. We thus investigated an alternative sampling scheme, based on a short dynamic at the start of the study and a short delayed scan. We again used the formalism of OSS to find the optimum mid scan time at around 3 h for the delayed scan and the sampling schedule of the early, short dynamic. With an initial 30-min dynamic study, accuracy and precision were similar to a continuous collection over 90–120 min for both K_1 and V_d (Figs. 9 and 10). The time requirements for the split session sampling scheme are similar to current Tl-201 rest/redistribution studies, and are thus clinically practical. Further, estimation of K_1 and V_d should eliminate the need for 24-h images, which may in fact reduce the total study time.

C. Effect of TTAC on OSS Accuracy

The OSS depends on the shape of the TTAC curve. Thus OSS for Tl-201 will vary depending on the exact shape of the TTAC for a particular subject and region, which is not normally know *a priori*. In this study we determined the OSS based only on TTAC for parameter set 1 and applied this OSS to all the other parameter sets, which were specifically chosen to cover a wide range of K_1 and V_d and, hence, a wide range of TTAC shapes (Fig. 3). The results shown in Figs. 7 and 8 demonstrate the validity of using a single OSS schedule for a wide range of TTAC's. No systematic difference in percentage error as a function of TTAC is seen between OSS and DynSS. Only CV for K_1 is increased by approximately 3%–4% for set 4 and set 5, which represent the extreme deviation from the average TTAC (set 1) used to generate the OSS (Fig. 3).

In this study we have concentrated on the sampling requirements for estimation of compartmental model rate constants. A further requirement is accurate activity estimation in the myocardium with a prerequisite for both accurate attenuation and scatter correction as well correction for partial volume effects. With the increased availability of transmission measurements on particularly multidetector SPECT systems and algorithms for scatter correction [21], [22], quantitative SPECT is becoming more feasible and practical and has in fact been applied to the dog studies used as the basis of this investigation. For compartmental modeling, the arterial plasma concentration of the tracer is also required. Ideally, this is obtained by frequent arterial blood sampling, which is, however, considered too invasive for routine clinical studies. It has been shown recently that population-based input functions calibrated with one or two blood samples can alleviate the need for full arterial sampling [28], and these techniques should also be applicable to Tl-201 studies.

V. Conclusions

In this study, we have developed a methodology determining total acquisition time and for optimizing sampling schedule for dynamic SPECT studies. When applied to dynamic SPECT Tl-201 model, it was found that for myocardial blood flow only, a 30-min scanning duration is sufficient. V_d estimation required an additional study at approximately 3 h, which avoided the need for prolonged continuous dynamic acquisition. Both K_1 and V_d can, thus, be determined with a clinically practical sampling schedule. This study also highlights that careful consideration needs to be given to total acquisition time to obtain reliable estimates of all parameters of interest, particularly for typical SPECT tracers with slow kinetic components. The method for determining OSS and total acquisition time applied here to Tl-201 should also be applicable to other SPECT tracers.

References

[1] H. Iida, H. Itoh, M. Nakazawa, J. Hatazawa, H. Nishimura, Y. Onishi, and K. Uemura, "Quantitative mapping of regional cerebral blood flow using iodine-123-IMP and SPECT," *J. Nucl. Med.*, vol. 35, pp. 2019–2030, 1994.

[2] H. Iida, H. Itoh, P. M. Bloomfield, M. Munaka, S. Higano, M. Murakami, A. Inugami, S. Eberl, Y. Aizawa, I. Kanno, and K. Uemura, "A method to quantitate cerebral blood flow using a rotating gamma camera and iodine-123 iodoamphetamine with one blood sampling," *Eur. J. Nucl. Med.*, vol. 21, pp. 1072–1084, 1994.

[3] Y. Onishi, Y. Yonekura, S. Nishizawa, F. Tanaka, H. Okazawa, K. Ishizu, T. Fujita, J. Konishi, and T. Mukai, "Noninvasive quantification of iodine-123-iomazenil SPECT," *J. Nucl. Med.*, vol. 37, pp. 374–378, 1996.

[4] A. M. Smith, G. T. Gullberg, P. E. Christian, and F. L. Datz, "Kinetic modeling of teboroxime using dynamic SPECT imaging in a canine model," *J. Nucl. Med.*, vol. 35, pp. 484–495, 1994.

[5] P. C. Chiao, E. P. Ficaro, F. Dayanikli, W. L. Rogers, and M. Schwaiger, "Compartmental analysis of technetium-99m-teboroxime

kinetics employing FST dynamic SPECT at rest and stress," *J. Nucl. Med.*, vol. 35, pp. 1254–1273, 1994.

[6] H. Iida, Y. Tamura, Y. Narita, S. Eberl, and Y. Ono, "Use of Tl-201 and SPECT for quantitative assessment of regional myocardial blood flow," *J. Nucl. Med.*, vol. 38, p. 165p, 1997.

[7] R. A. Hawkins, M. E. Phelps, and S. C. Huang, "Effects of temporal sampling, glucose metabolic rates, and disruptions of the blood-brain barrier on the FDG model with and without a vascular compartment: Studies in human brain tumors with PET," *J. Cereb. Blood Flow Metab.*, vol. 6, pp. 170–183, 1986.

[8] B. M. Mazoyer, R. H. Huesman, T. F. Budinger, and B. L. Knittel, "Dynamic PET data analysis," *J. Comput. Assist. Tomogr.*, vol. 10, pp. 645–653, 1986.

[9] J. Delforge, A. Syrota, and B. M. Mazoyer, "Experimental design optimization: Theory and application to estimation of receptor model parameters using dynamic positron emission tomography," *Phys. Med., Biol.*, vol. 34, pp. 419–435, 1989.

[10] S. Jovkar, A. C. Evans, M. Diksic, H. Nakai, and Y. L. Yamamoto, "Minimization of parameter estimation errors in dynamic PET: Choice of scanning schedules," *Phys. Med., Biol.*, vol. 34, pp. 895–908, 1989.

[11] X. Li and D. Feng, "Toward the reduction of dynamic image data in PET studies," *Comput. Meth., Programs Biomed.*, vol. 53, pp. 71–80, 1997.

[12] F. Mori and J. J. DiStefano, III, "Optimal nonuniform sampling interval and test input design for identification of physiological system from very limited data," *IEEE Trans. Automat. Contr.*, vol. AC-24, pp. 893–900, 1979.

[13] J. J. DiStefano, III, "Optimized blood sampling protocols and sequential design of kinetic experiments," *Amer. J. Physiol.*, vol. 240, pp. R259–R265, 1981.

[14] X. Li, D. Feng, and K. Chen, "Optimal image sampling schedule: A new effective way to reduce dynamic image storage space and functional image processing time," *IEEE Trans. Med. Imag.*, vol. 15, pp. 710–719, 1996.

[15] D. Feng, X. Li, and C. Siu, "Optimal sampling schedule design for positron emission tomography data acquisition," *Contr. Eng. Practice*, vol. 5, pp. 1759–1766, 1997.

[16] D. Feng, X. Wang, and H. Yan, "A computer simulation study on the input function sampling schedules in tracer kinetic modeling with positron emission tomography (PET)," *Comput. Meth., Programs Biomed.*, vol. 45, pp. 175–186, 1994.

[17] K. Ho-Shon, D. Feng, R. A. Hawkins, S. Meikle, M. Fulham, and X. Li, "Optimized sampling and parameter estimation for quantification in whole body PET," *IEEE Trans. Biomed. Eng.*, vol. 43, pp. 1021–1028, 1996.

[18] A. Chatziioannou, M. Dahlbom, and C. K. Hoh, "Studies on the use of transmission scans for whole body PET attenuation correction," *1993 IEEE Conf. Rec., Nuclear Science Symp., Medical Imaging Conf.*, vol. 2, 1993, pp. 1111–1115.

[19] Y. Onishi, Y. Yonekura, T. Mukai, S. Nishizawa, F. Tanaka, H. Okazawa, K. Ishizu, T. Fujita, H. Shibasaki, and J. Konishi, "Simple quantification of benzodiazepine receptor binding and ligand transport using Iodine-123-iomazenil and two SPECT scans," *J. Nucl. Med.*, vol. 36, pp. 1201–1210, 1995.

[20] S. R. Meikle, B. F. Hutton, and D. L. Bailey, "A transmission dependent method for scatter correction in SPECT," *J. Nucl. Med.*, vol. 35, pp. 360–367, 1994.

[21] Y. Narita, S. Eberl, H. Lida, B. F. Hutton, M. Braun, T. Nakamura, and G. Bautovich, "Monte Carlo and experimental evaluation of accuracy and noise properties of two scatter correction methods for SPECT," *Phys. Med., Biol.*, vol. 41, pp. 2481–2496, 1996.

[22] Y. Narita, H. Lida, and S. Eberl, "Monte Carlo evaluation of accuracy and noise properties of two scatter correction methods," *IEEE Conf. Rec., Nuclear Science Symp., Medical Imaging Conf.*, vol. 2, 1996, pp. 1434–1439.

[23] H. M. Hudson and R. S. Larkin, "Accelerated image reconstruction using ordered subsets of projection data," *IEEE Trans. Med. Imag.*, vol. 13, pp. 601–609, 1994.

[24] J. B. Bassingthwaighte, B. Winkler, and R. B. King, "Potassium and thallium uptake in dog myocardium," *J. Nucl. Med.*, vol. 38, pp. 264–274, 1997.

[25] R. E. Carson, "Parameter estimation in positron emission tomography," in *Positron Emission Tomography and Autoradiography*, M. E. Phelps, J. C. Mazziotta, and H. R. Schelbert, Eds. New York: Raven, 1986, pp. 347–390.

[26] W. H. Press, S. A. Teukolsky, W. T. Vetterling, and B. P. Flannery, *Numerical Recipes in C: The Art of Scientific Computing*, 2nd ed. Cambridge, U.K.: Cambridge Univ. Press, 1992.

[27] J. V. Beck and K. J. Arnold, *Parameter Estimation in Engineering and Science*. New York: Wiley, 1977.

[28] S. Eberl, A. R. Anayat, R. R. Fulton, P. K. Hooper, and M. J. Fulham, "Evaluation of two population-based input functions for quantitative neurologic FDG PET studies," *Eur. J. Nucl. Med.*, vol. 24, pp. 299–304, 1997.